

Dynamics of neural fields with exponential temporal kernel

Elham Shamsara · Marius E. Yamakou · Fatihcan
M. Atay · Jürgen Jost

Received: date / Accepted: date

Abstract In this paper, we consider the standard neural field equation with an exponential temporal kernel. We analyze the time-independent (static) and time-dependent (dynamic) bifurcations of the equilibrium solution and the emerging spatio-temporal wave patterns. We show that an exponential temporal kernel does not allow static bifurcations such as saddle-node, pitchfork, and in particular, static Turing bifurcations, in contrast to the Green's function used by Atay and Hutt (SIAM J. Appl. Math. 65: 644-666, 2004). However, the exponential temporal kernel possesses the important property that it takes into account finite memory of past activities of neurons, which the Green's function does not. Through a dynamic bifurcation analysis we give explicit Hopf (temporally non-constant, but spatially constant solutions) and Turing-Hopf (spatially and temporally non-constant solutions) bifurcation conditions on the parameter space which consists of the internal input current, the time delay rate of synapses, the ratio of excitatory to inhibitory synaptic weights, the coefficient of the exponential temporal kernel, and the transmission speed of neural signals.

Keywords Neural fields, exponential temporal kernel, leakage, transmission delays, bifurcation analysis, spatio-temporal patterns

Mathematics Subject Classification (2010) 92C20 · 37N25 · 37G10

1 Introduction

Neurons are the basic building cells of the brain. They are connected in dense networks and communicate with each other by transmitting neural information via their synapses [1]. Neural field theory considers populations of neurons embedded in a coarse-grained spatial area and neural field equations describe the spatio-temporal evolution of coarse grained variables like the firing rate activity in these populations of neurons [2]. Neural field models were first introduced by Wilson and Cowan

E. Shamsara · M. E. Yamakou · J. Jost

Max-Planck-Institut für Mathematik in den Naturwissenschaften, Inselstr. 22, 04103 Leipzig, Germany

E. Shamsara

Social Determinants of Health Research Center, Mashhad University of Medical Sciences, 91778-99191 Mashhad, Iran

Fatihcan M. Atay

Department of Mathematics, Bilkent University, 06800 Ankara, Turkey

J. Jost

Santa Fe Institute for the Sciences of Complexity, NM 87501, Santa Fe, USA

E-mail: elham.shamsara@mail.um.ac.ir

E-mail: yamakoumarius@gmail.com, Corresponding author

E-mail: f.atay@bilkent.edu.tr

E-mail: jost@mis.mpg.de

as a spatially extended version of Hopfield neural networks [2, 3]. A simplified model that could be mathematically treated in rather explicit form was developed by Amari [4], which consists of non-linear integro-differential equations. These equations play an important role also in other fields such as machine learning, which combines ideas from neural field modeling and model based recognition [5, 6].

Neural fields have seen significant progress in both theoretical and numerical studies over the recent years [7–14]. An important fact in neural field modeling is the consideration of axonal conduction delays arising from the finite speed of signals traveling along the axonal distance. Some recent and significant contributions to neural fields modeling with transmission delays are presented in [16–19]. In [16], a stability analysis is given for neural field equations in the presence of finite propagation speed and for a general class of connectivity kernels, and sufficient conditions for the stability of equilibrium solutions are given. It is shown that the non-stationary bifurcations of equilibria depend on the propagation delays and the connectivity kernel, whereas the stationary bifurcations depend only on the connectivity kernel. In [18], the stability of neural fields with a general connectivity kernel and space dependent transmission delays is analyzed. It is found that Turing instability occurs with local inhibition and lateral excitation, while wave instability occurs with local excitation and lateral inhibition. The standard field model of neural populations with propagation speed distribution of signal transmission speeds is considered in [19], where the effect of distributed speeds on the dynamical behavior is investigated. It is shown that the variance of the speed distribution affects the frequency of bifurcating periodic solutions and the phase speed of traveling waves. It is also shown that the axonal speed distributions lead to the increases of the traveling front speed. The results in [19] were extended in [17], where long-range feedback delays are considered in the standard neural field model. There, it is shown that in a reduced model delayed excitatory feedback generally facilitates stationary bifurcations and Turing patterns, while suppressing the bifurcation of periodic solutions and traveling waves. In case of oscillatory bifurcations, the variance of the distributed propagation and feedback delays affects the frequency of periodic solutions and the phase speed of traveling waves.

The objective of this work is to analytically and numerically study the static and dynamic bifurcations and spatio-temporal wave patterns generated by the classical neural field model with an *exponential* temporal kernel. This form of the temporal kernel is more general than the Green's function used in [16] and [20]. In [20] the temporal connectivity kernel is the product of an alpha function and the Heaviside function, which yields a function with the same properties as the Green's function, and thus yields the same characteristic polynomial as in [16]. We recall that the Green's function $G(t, t')$ is the solution to $LG(t, t') = \delta(t - t')$ satisfying the given boundary conditions, where L is a differential operator. This is a differential equation for G (or a partial differential equation if we are in more than one dimension), with a very specific source term on the right-and-side: the Dirac delta, which is an on-off function i.e., either 0 if $t \neq t'$ or ∞ if $t = t'$, and hence does not take into account finite memory of past activities of neurons. In contrast, in this paper, the derivative of the exponential temporal kernel tends to 0 as $t \rightarrow \infty$ and also decreases monotonically in finite time, meaning that it takes into account a finite memory of past activities of neurons, which the Green's function does not. Ref. [20] is quite inspiring for reducing a biologically more realistic microscopic model of leaky integrate-and-fire neurons with distance-dependent connectivity to an effective neural field model. Because of the type of kernels used there, two different neuron populations, excitatory and inhibitory ones, are needed to induce dynamic bifurcations. Here, we work with a Mexican hat type spatial kernel (which models short range excitation and mid range inhibition) and, as explained, an exponential temporal kernel, and we can therefore generate similar types of dynamic bifurcations as in [20] with only a single population.

Neural field models by intention ignore many details of the behavior of neurons and focus on collective patterns. The question then arises to what extent they are able to reproduce important

qualitative properties of large neuronal systems that have been proposed as relevant for understanding certain cognitive phenomena and to explain their dynamical emergence. The base state of neural fields is the zero state where nothing happens. This is of course not a biological state, and therefore, we should see how varying the values of relevant parameters that guide the collective behavior can produce biologically more plausible dynamics. Importantly, real biological networks do not show static behavior, even if spatially very inhomogeneous. In that regard, our version of neural field models with the biologically realistic and important assumption of transmission delays does not produce bifurcations to static inhomogeneous patterns. The most important qualitative neurobiological phenomenon rather seems to be a synchronized dynamics which is temporally varying, but in its most version might be spatially rather homogeneous. In our model, we can produce such a dynamic phenomenon through a Hopf bifurcation. Of course, a spatially homogeneous solution is only a rather coarse pattern. Therefore, it is reassuring to see that in our model, through a Turing-Hopf bifurcation, we can also produce patterns that are both temporally and spatially varying. The next question would then be which qualitative types of spatiotemporal dynamics are observed in real neuronal networks and which spatiotemporal patterns our neural field model, or perhaps an extension thereof, is capable of generating.

This paper is organized as follows: In Sect. 2, we present the model equation and obtain its equilibrium solution. Sect. 3 is devoted to the static bifurcation analysis of the equilibrium solution. In Sect. 4, we investigate dynamic bifurcations of the equilibrium solution and the ensuing patterns of traveling waves. We conclude with some remarks in Sect. 5.

2 The model and the equilibrium solution

We consider a neural field model represented by an infinite-dimensional dynamical system in the form of an integro-differential equation [21–24], with axonal conduction delay [25–27]. In this equation, the position of a neuron at time t is given by a spatial variable x , in the literature usually considered to be continuous in \mathbb{R} or \mathbb{R}^2 . The state of the neural field, $v(x, t)$ (membrane potential), evolves according to

$$v(x, t) = \int_{-\infty}^t \left[\kappa(t-s)S(x, s) + I_1(x, s) \right] ds - \frac{1}{\tau} \int_{-\infty}^t v(x, s) ds. \quad (2.1)$$

Here, $v(x, t)$ is a potential response function that represents the local activity of a population of neurons at position x and time t , and $I_1(x, t)$ is an external input current. The first integral converts the incoming pulse activity S of the neuron at x into its state by convolution with a temporal kernel (impulse response function) κ . The second integral is a decay or leakage term, with a time constant $\tau > 0$ arising from the temporal decay rate of synapses. In this paper, we take the past activity of neurons into account for the impulse response using an *exponential* temporal kernel. In [16], such a kernel was taken as the Green's function of a first order differential operator. Here, in order to be able to carry out a detailed bifurcation analysis depending on that kernel, we use a more explicit form, namely an exponential decay:

$$\kappa(t-s) = \begin{cases} \alpha_1 e^{-\alpha_2(t-s)} & \text{if } t-s \geq 0, \\ 0 & \text{if } t-s < 0, \end{cases} \quad (2.2)$$

where α_1 and α_2 are positive constants, with a normalization condition requiring that the integral of the kernel be 1, i.e. $\alpha_1 = \alpha_2 := \alpha$. Such kernels are standard in the neuroscience literature and are usually called α -functions (see e.g. [15]): It is worth noting that even though the exponential kernel used in this work reduces to the kernel used in [16] as $\alpha \rightarrow \infty$, our bifurcations cannot, in general, automatically reduce to those in [16]. The presence of a leakage term (which is neglected in

[16]), characterized by a temporal decay rate parameter $\tau > 0$ in our model, does not allow for such a reduction.

The crucial idea in neural field models is that the incoming activity $S(x, t)$ is obtained by a spatial convolution via an integral with some convolution kernel $J(x, y)$, that is,

$$S(x, t) = c \int_{\Omega} J(x, y) F\left(v(y, t - \frac{d(x, y)}{\nu})\right) dy + I_2(x, t). \quad (2.3)$$

Here, $c > 0$ is some constant that involves various temporal and spatial scales, Ω is the spatial domain which is usually taken as \mathbb{R} or \mathbb{R}^2 in the literature, although other choices, like \mathbb{R}^3 or S^2 , are neuro-biologically plausible and mathematically tractable. The synaptic weight function J typically describes local excitation–lateral inhibition or local inhibition–lateral excitation. The function F is a transfer function (for instance a sigmoid or a Heaviside function $H(v - v_{th})$, for some threshold v_{th} ; however, later on, F needs to be smooth), $I_2(x, t)$ is an internal input current, $d(x, y)$ is the distance between x and y (for instance the Euclidean distance $|x - y|$) and ν is the transmission speed of neural signals. Thus, a finite transmission speed introduces a distance-dependent transmission delay, which approaches 0 as $\nu \rightarrow \infty$. We also assume a homogeneous field where the connectivity $J(x, y)$ depends only on the distance $|x - y|$, and so we replace $J(x, y)$ by an even function $J(x - y)$. In our numerical investigations we will use the following spatial convolution kernel and sigmoid transfer function [29]:

$$J(x - y) = \frac{a_e}{2} e^{-|x-y|} - \frac{a_i r}{2} e^{-|x-y|r}, \quad (2.4)$$

$$F(v) = \frac{1}{1 + \exp(-1.8(v - 3))}, \quad (2.5)$$

where a_e and a_i respectively denote the excitatory and inhibitory synaptic weights and $r := a_e/a_i$, gives the relation of excitatory and inhibitory spatial connectivity ranges. J has the well established Mexican hat shape, modeling short range excitation and mid range inhibition, and decay to 0 as $|x - y| \rightarrow \infty$.

Differentiating (2.1) with respect to t yields

$$\frac{d}{dt} v(x, t) = \int_{-\infty}^t \frac{d\kappa(t-s)}{dt} S(x, s) ds - \frac{1}{\tau} v(x, t) + \alpha S(x, t) + I_1(x, t) \quad (2.6)$$

Inserting (2.2) and (2.3) in (2.6) gives

$$\begin{aligned} \frac{d}{dt} v(x, t) = & -\alpha^2 c \int_{-\infty}^t e^{-\alpha(t-s)} \int_{\Omega} J(x - y) F\left(v(y, s - \frac{d(x, y)}{\nu})\right) dy ds - \alpha^2 \int_{-\infty}^t e^{-\alpha(t-s)} I_2(x, s) ds \\ & - \frac{1}{\tau} v(x, t) + \alpha c \int_{\Omega} J(x - y) F\left(v(y, t - \frac{d(x, y)}{\nu})\right) dy + \alpha I_2(x, t) + I_1(x, t). \end{aligned} \quad (2.7)$$

In order to analyze the dynamic behavior of (2.7), we assume a constant internal and external input currents, i.e $I_1(x, s) = E$, $I_2(x, s) = I_0$, and a constant solution

$$v(x, t) = v_0. \quad (2.8)$$

Substituting into (2.7) shows that v_0 satisfies the fixed point equation

$$v_0 + \alpha \tau c F(v_0) \int_{\Omega} J(x - y) dy + \alpha \tau I_0 - \alpha \tau I_0 - \alpha \tau c F(v_0) \int_{\Omega} J(x - y) dy + E = 0, \quad (2.9)$$

which is satisfied by the fixed point (equilibrium solution)

$$v_0 = -E. \quad (2.10)$$

In the following sections, we study the static and dynamic bifurcations of the equilibrium solution $v_0 = -E = 0.55$.

3 Static bifurcation analysis of the equilibrium solution

For rest of this paper, we take $\Omega = \mathbb{R}$ for simplicity. To obtain the parametric region of the stability of the equilibrium solution (2.10), we linearize the integro-differential equation (2.7) around the equilibrium solution $v_0 = -E$. Let $w(x, t) = v(x, t) - v_0$. Then,

$$\begin{aligned} \frac{d}{dt}w(x, t) = & -\alpha^2 c \int_{-\infty}^t e^{-\alpha(t-s)} \int_{-\infty}^{\infty} J(x-y) \left[F(v_0) + F'(v_0)w(y, s - \frac{d(x, y)}{\nu}) \right] dy ds \\ & - \alpha I_0 - \frac{1}{\tau}w(x, t) + \frac{v_0}{\tau} + \alpha c \int_{-\infty}^{\infty} J(x-y) \left[F(v_0) + F'(v_0)w(y, t - \frac{d(x, y)}{\nu}) \right] dy + \alpha I_0 + E, \end{aligned} \quad (3.1)$$

which simplifies to

$$\begin{aligned} \frac{d}{dt}w(x, t) = & -\alpha^2 c F'(v_0) \int_{-\infty}^t e^{-\alpha(t-s)} \int_{-\infty}^{\infty} J(x-y) w(y, s - \frac{d(x, y)}{\nu}) dy ds \\ & - \frac{1}{\tau}w(x, t) + \frac{v_0}{\tau} + \alpha c F'(v_0) \int_{-\infty}^{\infty} J(x-y) w(y, t - \frac{d(x, y)}{\nu}) dy + E, \end{aligned} \quad (3.2)$$

where the notation $F'(v_0)$ denotes $\frac{dF}{dv}(v_0)$. To check the stability of the equilibrium solution, we substitute the general Fourier-Laplace ansatz for linear integro-differential equations

$$w(x, t) = e^{\lambda t} e^{ikx}, \quad \lambda \in \mathbb{C}, k \in \mathbb{R}, \quad (3.3)$$

into (3.2) to get

$$\begin{aligned} (\tau\lambda + 1)e^{\lambda t} e^{ikx} = & -\alpha^2 c \tau F'(v_0) \int_{-\infty}^t e^{-\alpha(t-s)} e^{\lambda s} \int_{-\infty}^{\infty} J(x-y) e^{iky} e^{-\lambda \frac{d(x, y)}{\nu}} dy ds \\ & + \alpha c \tau F'(v_0) e^{\lambda t} \int_{-\infty}^{\infty} J(x-y) e^{iky} e^{-\lambda \frac{d(x, y)}{\nu}} dy + E + v_0. \end{aligned} \quad (3.4)$$

From (2.10), we note that $E + v_0 = 0$ in (3.4). The first integral in (3.4) is independent of y , so

$$\int_{-\infty}^t e^{-\alpha(t-s)} e^{\lambda s} ds = \frac{1}{\alpha + \lambda} e^{\lambda t}. \quad (3.5)$$

By making a change of variable: $z = x - y$ in (3.4), and considering $\lambda \neq -\alpha$, we obtain the linear variational equation as

$$\tau\lambda + 1 = \alpha c \tau F'(v_0) \left(\frac{\lambda}{\alpha + \lambda} \right) \int_{-\infty}^{\infty} J(z) e^{-\lambda \frac{|z|}{\nu}} e^{-ikz} dz. \quad (3.6)$$

For static bifurcations, that is, for bifurcations leading to temporally constant solutions, we must have $\lambda = 0$ [16]. However, it is easy to see that $\lambda = 0$ is not a solution of (3.6). Therefore, static bifurcations (such as saddle-node and pitchfork bifurcations) cannot occur, and hence, in particular, static Turing patterns [28, 29] are not possible with an exponential temporal kernel.

We next give a sufficient condition for the asymptotic stability of the equilibrium solution v_0 . We make use of the following lemma from [16].

Lemma 1 *Let $L(\lambda)$ be a polynomial whose roots have non-positive real parts. Then $|L(\sigma + i\omega)| \geq |L(i\omega)|$ for all $\sigma \geq 0$ and $\omega \in \mathbb{R}$.*

Proof : See [16]. □

Theorem 1 Let $D := |\beta| \int_{-\infty}^{\infty} |J(z)| dz$, where $\beta = \alpha \tau F'(v_0)$. If

$$D < \min_{\omega \in \mathbb{R}} |L(i\omega)|, \quad (3.7)$$

then v_0 is asymptotically stable. In particular, the condition

$$D < 1 \quad (3.8)$$

is sufficient for the asymptotic stability of v_0 .

Proof : In the ansatz $w(x, t) = e^{\lambda t} e^{ikx}$, let $\lambda = \sigma + i\omega$, where σ and ω are real numbers. We will prove that $\sigma < 0$ if (3.7) holds. Suppose by the way of contradiction that (3.7) holds but $\sigma \geq 0$. From (3.6) it follows that

$$\begin{aligned} |L(\sigma + i\omega)| &= |\beta| \left| \frac{\sigma + i\omega}{\alpha + \sigma + i\omega} \right| \left| \int_{-\infty}^{\infty} J(z) e^{-(\sigma + i\omega) \frac{|z|}{\nu}} e^{-ikz} dz \right| \\ &\leq |\beta| \left| \frac{\sigma + i\omega}{\alpha + \sigma + i\omega} \right| \int_{-\infty}^{\infty} |J(z)| \left| e^{-(\sigma + i\omega) \frac{|z|}{\nu}} \right| dz \\ &\leq |\beta| \left| \frac{\sigma + i\omega}{\alpha + \sigma + i\omega} \right| \int_{-\infty}^{\infty} |J(z)| dz. \end{aligned}$$

Since $\alpha > 0$, we have $\left| \frac{\sigma + i\omega}{\alpha + \sigma + i\omega} \right| < 1$, which means

$$|L(\sigma + i\omega)| \leq |\beta| \int_{-\infty}^{\infty} |J(z)| dz. \quad (3.9)$$

By Lemma 1,

$$|L(i\omega)| \leq |L(\sigma + i\omega)| \leq |\beta| \int_{-\infty}^{\infty} |J(z)| dz =: D, \quad (3.10)$$

for some $\omega \in \mathbb{R}$. This, however, contradicts (3.7). Thus $\sigma < 0$, and the equilibrium solution v_0 is asymptotically stable. This proves the first statement of the theorem. Since by (3.6), $L(\lambda) = \tau\lambda + 1$, one has $|L(i\omega)|^2 = 1 + \tau^2\omega^2$. Hence, if (3.8) is satisfied, then

$$D^2 < 1 \leq 1 + \tau^2\omega^2 = |L(i\omega)|^2 \quad (3.11)$$

for all $\omega \in \mathbb{R}$, which is a sufficient condition for stability by (3.8).

It is worth noting that an exponential temporal kernel has the advantage of taking into account the finite memory of past activities of neurons, which the Green's function considered in [16] does not. An exponential temporal kernel is therefore more general in this respect than the Green's function, since the memory decreases exponentially and converges to the Dirac delta function as time tends to infinity. In Fig.1(a)-(c), we present the bifurcation diagrams showing the regions of stability and instability of the equilibrium solution v_0 . In panels, the quantity $D := |\beta| \int_{-\infty}^{\infty} |J(z)| dz$ is plotted against the bifurcation parameters α , r , and τ .

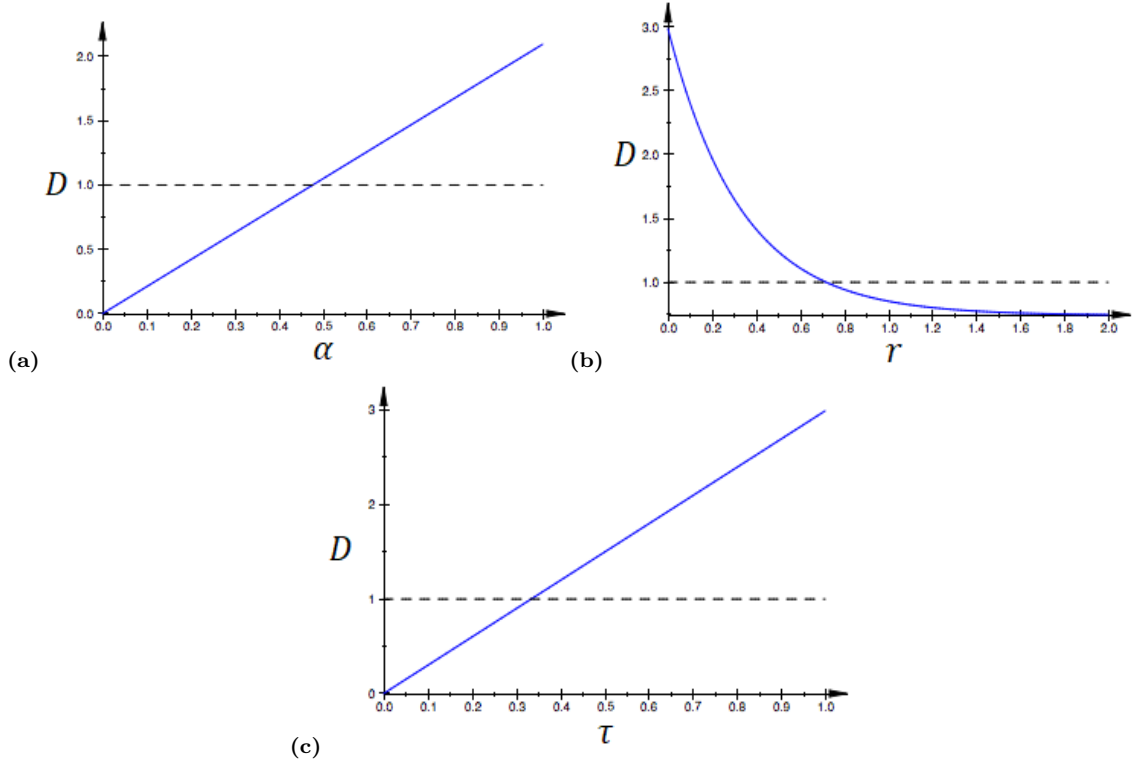


Figure 1: The blue curves represent the quantity D from Theorem 1 plotted against the bifurcation parameters: α in (a) with $\tau = 0.7$, $r = 0.5$; r in (b) with $\alpha = 1.0$, $\tau = 0.7$; and τ in (c) with $\alpha = 1.0$, $r = 0.5$. The intervals of $\alpha \in (0.0, 0.48)$, $r \in (0.0, 0.73)$, and $\tau \in (0.0, 0.33)$ in which the blue curves are below the dashed horizontal line fulfill the sufficient condition of asymptotic stability of the equilibrium solution $v_0 = 0.55$, following Theorem 1. Other parameters are fixed at: $c = 15.0$, $a_i = 10.0$, $a_e = ra_i$.

4 Dynamic bifurcation analysis of the equilibrium solution

In the previous section, we have seen that static bifurcations are not possible since $\lambda = 0$ is not a solution of (3.6). In this section, we investigate the conditions for oscillatory (dynamic) bifurcations. In case of a homogeneous and isotropic neural field, we use the kernel function J and the sigmoid transfer function F in (2.4) and (2.5), respectively. Equation (3.6) can then be written as

$$\begin{aligned}
 \tau\lambda^2 + (\tau\alpha + 1)\lambda + \alpha &= \alpha c \tau F'(v_0) \lambda \int_{-\infty}^{\infty} J(z) e^{-\lambda \frac{|z|}{\nu}} e^{-ikz} dz \\
 &= \beta \lambda \left[\int_{-\infty}^{\infty} \left(\frac{a_e}{2} e^{-|z|} - \frac{a_i r}{2} e^{-|z|r} \right) e^{-\lambda \frac{|z|}{\nu}} e^{-ikz} dz \right] \\
 &= \beta \lambda \left[a_e \frac{1}{(1 + \frac{\lambda}{\nu}) + ik} - a_i r \frac{1}{(r + \frac{\lambda}{\nu}) + ik} \right] \\
 &= \beta \lambda \left[a_e \frac{1 + \frac{\lambda}{\nu}}{(1 + \frac{\lambda}{\nu})^2 + k^2} - a_i r \frac{r + \frac{\lambda}{\nu}}{(r + \frac{\lambda}{\nu})^2 + k^2} \right] \\
 &\quad - i\beta \lambda k \left[\frac{a_e}{(1 + \frac{\lambda}{\nu})^2 + k^2} - \frac{a_i r}{(r + \frac{\lambda}{\nu})^2 + k^2} \right]. \tag{4.1}
 \end{aligned}$$

Comparing the real parts of the two sides of (4.1), we get

$$\begin{aligned} & \left[k^2 + \left(r + \frac{\lambda}{\nu} \right)^2 \right] \left[k^2 + \left(1 + \frac{\lambda}{\nu} \right)^2 \right] \left(\tau \lambda^2 + (\tau \alpha + 1) \lambda + \alpha \right) \\ & - a_e \beta \lambda \left(1 + \frac{\lambda}{\nu} \right) \left[k^2 + \left(r + \frac{\lambda}{\nu} \right)^2 \right] + r a_i \beta \lambda \left(r + \frac{\lambda}{\nu} \right) \left[k^2 + \left(1 + \frac{\lambda}{\nu} \right)^2 \right] = 0, \end{aligned} \quad (4.2)$$

which is a polynomial of degree six in λ . By tuning the parameters r , τ or α , a critical point is eventually reached at $k = k_c$ in which the real part of the corresponding eigenvalue $\lambda(k_c)$ of (4.2) becomes zero. From this critical point, one gets the critical wave-number k_c and the critical frequency $\omega_c = \text{Im } \lambda(k_c)$. The case $k_c = 0$ and $\omega_c \neq 0$ corresponds to a Hopf bifurcation [30–32], and the case $k_c \neq 0$ and $\omega_c \neq 0$ to a Turing-Hopf bifurcation [28, 33, 34]. We investigate both cases in more detail.

4.1 Hopf bifurcation

We search for conditions for Hopf bifurcation, i.e., when $k_c = 0$ and the real part of the corresponding eigenvalue $\lambda|_{(k_c=0)}$ becomes zero, while $\omega_c = \text{Im } \lambda|_{(k_c=0)} \neq 0$. To obtain these conditions, we insert $k = k_c = 0$ in (4.2) and obtain

$$q_6 \lambda^6 + q_5 \lambda^5 + q_4 \lambda^4 + q_3 \lambda^3 + q_2 \lambda^2 + q_1 \lambda + q_0 = 0, \quad (4.3)$$

where

$$\begin{cases} q_6 = \tau, \\ q_5 = 2\tau(r+1)\nu + \alpha\tau + 1, \\ q_4 = 2\tau(0.5 + 0.5r^2 + 2r)\nu^2 + ((a_i\beta + 2\alpha\tau + 2)r + 2\alpha\tau - a_e\beta + 2)\nu + \alpha, \\ q_3 = 2\tau(r+1)r\nu^3 + [(\alpha\tau + a_i\beta + 1)r^2 + 4(\alpha\tau + 1 - (a_e - a_i)\beta)r \\ \quad + \alpha\tau + 1 - a_e\beta]\nu^2 + 2\alpha(r+1)\nu, \\ q_2 = \tau r^2 \nu^4 + [(2\alpha\tau + 2 - (a_e - 2a_i)\beta)r^2 + (2\alpha\tau + 2 + (-2a_e + a_i)\beta)r]\nu^3 \\ \quad + \alpha(1 + r^2 + 4r)\nu^2, \\ q_1 = (\alpha\tau + 1 - (a_e - a_i)\beta)r^2 \nu^4 + 2\alpha(r+1)r\nu^3, \\ q_0 = \alpha\nu^4 r^2. \end{cases} \quad (4.4)$$

By simplifying (4.3), one can already get two of its six solutions, given by

$$\begin{cases} \lambda_1 = -\nu, \\ \lambda_2 = -\nu r. \end{cases} \quad (4.5)$$

The remaining four solutions of (4.3) should then satisfy the a polynomial equation of degree four:

$$p_4 \lambda^4 + p_3 \lambda^3 + p_2 \lambda^2 + p_1 \lambda + p_0 = 0, \quad (4.6)$$

where

$$\begin{cases} p_4 = \tau, \\ p_3 = \tau\nu r + \alpha\tau + \tau\nu + 1, \\ p_2 = \nu a_i \beta r + \nu \alpha r \tau + \tau \nu^2 r - \nu a_e \beta + \nu \alpha \tau + \alpha + (r+1)\nu, \\ p_1 = -a_e \beta \nu^2 r + a_i \beta \nu^2 r + \alpha \nu^2 r \tau + \alpha \nu r + \nu^2 r + \alpha \nu, \\ p_0 = \alpha \nu^2 r. \end{cases} \quad (4.7)$$

Substituting $\lambda = i\omega_c$ in (4.6) and separating the real and imaginary parts yields

$$\begin{cases} a_4\omega_c^4 + a_2\omega_c^2 + a_0 = 0, \\ b_3\omega_c^3 + b_1\omega_c = 0, \end{cases} \quad (4.8)$$

where

$$\begin{cases} a_4 = \tau, \\ a_2 = -\nu a_i \beta r - \nu \alpha r \tau - \tau \nu^2 r + \nu a_e \beta - \nu \alpha \tau - \alpha - (r+1)\nu, \\ a_0 = \alpha \nu^2 r, \\ b_3 = -\tau \nu r - \alpha \tau - \tau \nu - 1, \\ b_1 = -a_e \beta \nu^2 r + a_i \beta \nu^2 r + \alpha \nu^2 r \tau + \alpha \nu r + \nu^2 r + \alpha \nu. \end{cases} \quad (4.9)$$

We obtain ω_c from the second equation of (4.8) as

$$\omega_c^2 = -\frac{b_1}{b_3}. \quad (4.10)$$

Substituting (4.10) in the first equation of (4.8) gives $\nu = \nu(r, \tau, \alpha, \beta, a_e, a_i)$ as

$$g(\nu) := \nu^4 + \frac{u_3}{u_4}\nu^3 + \frac{u_2}{u_4}\nu^2 + \frac{u_1}{u_4}\nu + \frac{u_0}{u_4} = 0, \quad (4.11)$$

where

$$\begin{cases} u_4 = r^2 \tau^2 (r+1) (\alpha \tau + 1 - \beta(a_e - a_i)), \\ u_3 = \tau ((\alpha \tau + a_i \beta + 1) r^3 + (2\alpha \tau + 2) r^2 + (-a_e \beta + \alpha \tau + 1) r) (\alpha \tau - \beta(a_e - a_i) + 1), \\ u_2 = (\alpha \tau (a_i \beta + \alpha \tau + 1) r^3 + (a_i \beta + \alpha \tau + 1) (\tau^2 \alpha^2 - (-3 + (a_e - a_i) \beta) \alpha \tau + 1 + (-a_e + a_i) \beta) r^2 \\ \quad + (-a_e \beta + \alpha \tau + 1) (\tau^2 \alpha^2 - (-3 + (a_e - a_i) \beta) \alpha \tau + 1 + (-a_e + a_i) \beta) r + \alpha \tau (-a_e \beta + \alpha \tau + 1)), \\ u_1 = \alpha (\alpha \tau + 1) ((a_i \beta + \alpha \tau + 1) r^2 + (2\alpha \tau + 2 + (-2a_e + 2a_i) \beta) r + \alpha \tau - a_e \beta + 1), \\ u_0 = \alpha^2 (\alpha \tau + 1) (r+1). \end{cases} \quad (4.12)$$

Proposition 1 *If $(\alpha \tau + 1 - \beta(a_e - a_i)) < 0$, then (4.11) has at least one positive root.*

Proof : We have $u_0 > 0$ which implies that $g(0) = \frac{u_0}{u_4} < 0$ whenever $(\alpha \tau + 1 - \beta(a_e - a_i)) < 0$. And since $\lim_{\nu \rightarrow \infty} g(\nu) = +\infty$, then by the continuity of g , there exists a ν_0 in $(0, \infty)$ such that $g(\nu_0) = 0$. \square

From (4.9), since we have $b_3 < 0$, b_1 must be positive, so that the right hand side of (4.10) is positive. The positivity of b_1 implies that

$$\nu [\beta(a_e - a_i) - (\alpha \tau + 1)] < \frac{\alpha(1+r)}{r}.$$

But if $[\alpha \tau + 1 - \beta(a_e - a_i)] < 0$, then $[\beta(a_e - a_i) - (\alpha \tau + 1)] > 0$, which ensures that

$$\nu < \frac{\alpha(1+r)}{r[\beta(a_e - a_i) - (\alpha \tau + 1)]}. \quad (4.13)$$

The positive solutions of (4.11) correspond to the substitution of the values of ω_c from (4.10). Thus, at the positive solutions, the Hopf bifurcation occurs in the parametric region satisfying (4.13). In other words, the relation in (4.13) provides the parametric region in which a Hopf bifurcation occurs if the value of ω_c in (4.10) also satisfies the first equation in (4.8). In the sequel, we corroborate the above theoretical results on Hopf bifurcation with numerical simulations, where the parameter

values of β , a_e , a_i , α , and τ are chosen such that $\beta(a_e - a_i) - (\alpha\tau + 1) > 0$.

In Fig.2, for example, we fix the parameters $a_e = 18.0$, $a_i = 10.0$, $c = 15.0$ and compute the range of values of the bifurcation parameters α and τ for which $\beta(a_e - a_i) - (\alpha\tau + 1) > 0$. Fig.2(a) and (b) show that $\beta(a_e - a_i) - (\alpha\tau + 1) > 0$ if $\alpha \in (0.8, 5.0)$ and $\tau \in (0.6, 5.0)$, respectively. In Fig.2(c)-(e), the gray area represents the region of the parameter spaces where (4.13) holds. The parts of blue curves that lie in the gray region represent the Hopf bifurcation curves because they satisfy (4.13) and (4.11) simultaneously. We observe that the vertical boundary of the gray region in Fig.2(c) and (d) exactly corresponds to the minimum value of α and τ in Fig.2(a) and (b), respectively, where $\beta(a_e - a_i) - (\alpha\tau + 1) > 0$.

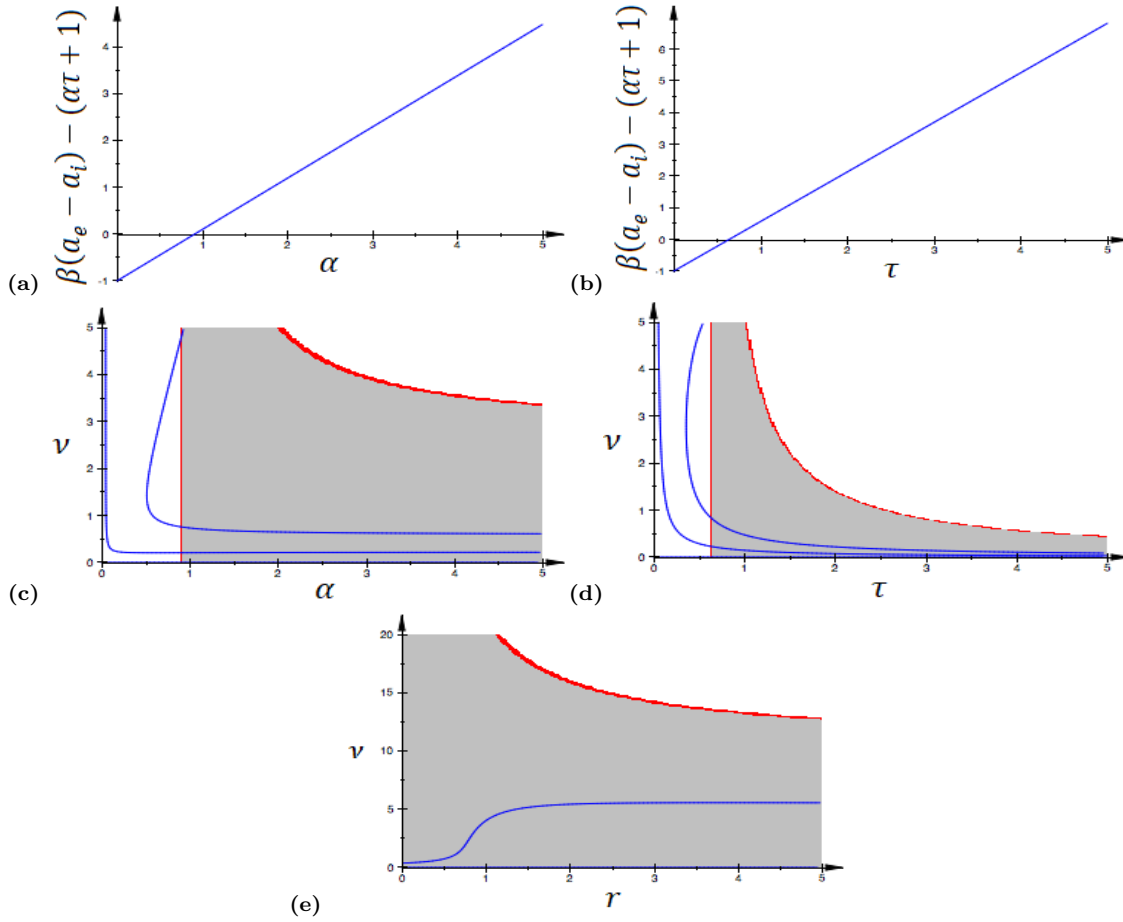


Figure 2: Panels (a) and (b) with show that interval of $\alpha \in (0.8, 5.0)$ and $\tau \in (0.6, 5.0)$ for which $\beta(a_e - a_i) - (\alpha\tau + 1) > 0$, respectively. In panels (c)-(e), the blue curves represent the solutions of (4.11) in the parameter spaces α - ν , τ - ν , and r - ν , respectively. The gray areas represent the region of the parameter spaces where (4.13) holds. The parts of blue curves that lie in the gray region represent the Hopf bifurcation curves because they satisfy (4.13) and (4.11) simultaneously. In (a): $\tau = 0.7$. In (b): $\alpha = 1.0$. In (c): $\tau = 0.7$, $r = 0.5$. In (d): $\alpha = 1.0$, $r = 0.5$, In (e): $\alpha = 1.0$, $\tau = 0.7$. In all panels, the other parameter values are: $c = 15.0$, $a_i = 10.0$, $a_e = ra_i$, $v_0 = 0.55$, $\beta = \alpha c \tau F'(v_0)$.

Fig.3 displays the space-time pattern of the corresponding Hopf bifurcation. Here, the values of r and ν are chosen on the Hopf bifurcation curve in Fig.2(e).

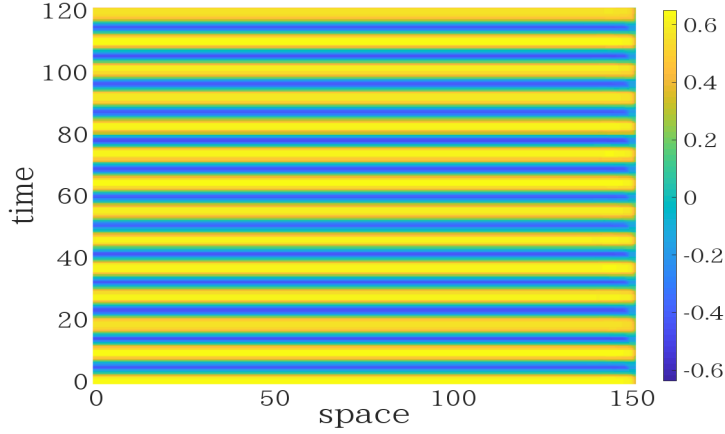


Figure 3: Space-time plot color coded by the membrane potential $v(x, t)$ of the Hopf instability leading to periodic oscillations of a spatially constant solutions, obtained for the Gaussian connectivity kernel. The initial conditions are chosen randomly from a uniform distribution on $[v_0 - 0.1, v_0 + 0.1]$. Other parameters are fixed at $a_i = 10.0$, $r = 0.5$, $a_e = ra_i$, $\alpha = 1.0$, $\nu = 0.79$, $\tau = 0.7$, $c = 15.0$, and $k = 0$.

4.2 Turing-Hopf bifurcation

The conditions for a Turing-Hopf bifurcation, at some critical value $k_c \neq 0$, require that $\lambda = \pm i\omega$ with $\omega \neq 0$. Inserting $\lambda = i\omega$ in (3.6), we obtain

$$L(i\omega) := 1 + i\tau\omega = \beta \left(\frac{i\omega}{\alpha + i\omega} \right) \int_{-\infty}^{\infty} J(z) e^{-i\omega \frac{|z|}{\nu}} e^{ikz} dz, \quad (4.14)$$

which yields upon expansion,

$$\begin{aligned} \beta \frac{\omega^2 + i\alpha\omega}{\alpha^2 + \omega^2} \int_{-\infty}^{\infty} J(z) e^{-i\omega \frac{|z|}{\nu}} \cos(kz) dz &= \beta \frac{\omega^2 + i\alpha\omega}{\alpha^2 + \omega^2} \int_{-\infty}^{\infty} J(z) \left[\cos\left(\frac{\omega|z|}{\nu}\right) - i \sin\left(\frac{\omega|z|}{\nu}\right) \right] \cos(kz) dz \\ &= \frac{\beta}{2} \frac{\omega^2 + i\alpha\omega}{\alpha^2 + \omega^2} \int_{-\infty}^{\infty} J(z) \left[\cos\left(\frac{\omega|z|}{\nu} + k|z|\right) + \cos\left(\frac{\omega|z|}{\nu} - k|z|\right) \right] dz \\ &\quad - \frac{i\beta}{2} \frac{\omega^2 + i\alpha\omega}{\alpha^2 + \omega^2} \int_{-\infty}^{\infty} J(z) \left[\sin\left(\frac{\omega|z|}{\nu} + k|z|\right) + \sin\left(\frac{\omega|z|}{\nu} - k|z|\right) \right] dz \\ &= \frac{\beta}{2} \frac{\omega^2 + i\alpha\omega}{\alpha^2 + \omega^2} \int_{-\infty}^{\infty} J(z) \left[e^{i|z|(\frac{\omega}{\nu} + k)} + e^{i|z|(\frac{\omega}{\nu} - k)} \right] dz. \end{aligned} \quad (4.15)$$

By substituting the power series

$$e^{i|z|(\frac{\omega}{\nu} \pm k)} = \sum_{n=0}^{\infty} \frac{i^n (\frac{\omega}{\nu} \pm k)^n}{n!} |z|^n,$$

(4.15) is written as

$$\frac{\beta}{2} \frac{\omega^2 + i\alpha\omega}{\alpha^2 + \omega^2} \int_{-\infty}^{\infty} J(z) \sum_{n=0}^{\infty} \frac{i^n}{n!} \left[\left(\frac{\omega}{\nu} + k \right)^n + \left(\frac{\omega}{\nu} - k \right)^n \right] |z|^n dz. \quad (4.16)$$

We define J_n as

$$J_n := \int_{-\infty}^{\infty} J(z) |z|^n dz. \quad (4.17)$$

Substituting (4.17) into (4.16) yields

$$L(i\omega) = \beta \frac{\omega^2 + i\alpha\omega}{\alpha^2 + \omega^2} \left[J_0 + i\frac{\omega}{\nu} J_1 - \frac{1}{2!} \left(k^2 + \frac{\omega^2}{\nu^2} \right) J_2 + \dots \right]. \quad (4.18)$$

Equating the right-hand side of (4.18) to the left-hand side of (4.14), we get

$$1 + i\tau\omega = \beta \frac{\omega^2 + i\alpha\omega}{\alpha^2 + \omega^2} \left[J_0 + i\frac{\omega}{\nu} J_1 - \frac{1}{2!} \left(k^2 + \frac{\omega^2}{\nu^2} \right) J_2 + \dots \right]. \quad (4.19)$$

Equating the real parts of both sides in (4.19), and similarly with the imaginary parts, and considering $\omega \neq 0$ (a Turing-Hopf bifurcation condition), we have

$$\begin{cases} 1 = \frac{\beta}{\alpha^2 + \omega^2} \left[\omega^2 J_0 - \alpha\omega \left(\frac{\omega}{\nu} J_1 \right) - \omega^2 \frac{1}{2!} \left(k^2 + \frac{\omega^2}{\nu^2} \right) J_2 + \dots \right], \\ \tau = \frac{\beta}{\alpha^2 + \omega^2} \left[\alpha J_0 + \omega \left(\frac{\omega}{\nu} J_1 \right) - \frac{1}{2!} \alpha \left(\left(k^2 + \frac{\omega^2}{\nu^2} \right) J_2 \right) + \dots \right]. \end{cases} \quad (4.20)$$

From (4.20) we have

$$\frac{\tau}{\alpha J_0 + \frac{\omega^2}{\nu} J_1 - \frac{\alpha}{2} \left(k^2 + \frac{\omega^2}{\nu^2} \right) J_2} = \frac{\beta}{\alpha^2 + \omega^2} = \frac{1}{\omega^2 J_0 - \alpha \frac{\omega^2}{\nu} J_1 - \frac{\omega^2}{2} \left(k^2 + \frac{\omega^2}{\nu^2} \right) J_2}, \quad (4.21)$$

which gives

$$\alpha J_0 + \frac{\omega^2}{\nu} J_1 - \frac{\alpha}{2} \left(k^2 + \frac{\omega^2}{\nu^2} \right) J_2 = \tau \omega^2 J_0 - \tau \alpha \frac{\omega^2}{\nu} J_1 - \tau \frac{\omega^2}{2} \left(k^2 + \frac{\omega^2}{\nu^2} \right) J_2. \quad (4.22)$$

After substituting (2.4) into (4.17), the convergent improper integrals J_n ($n = 0, 1, 2$) are calculated and explicitly given as

$$\begin{aligned} J_0 &= -a_i + a_e, \\ J_1 &= \frac{ra_e - a_i}{r}, \\ J_2 &= \frac{2(r^2 a_e - a_i)}{r^2}. \end{aligned} \quad (4.23)$$

Substituting (4.23) into (4.22), we obtain

$$\begin{aligned} & \frac{\tau}{\nu^2} \left(\frac{r^2 a_e - a_i}{r^2} \right) \omega^4 + \left[\tau(a_i - a_e) + \left(\tau k^2 - \frac{\alpha}{\nu^2} \right) \left(\frac{r^2 a_e - a_i}{r^2} \right) + \left(\frac{\alpha\tau + 1}{\nu} \right) \left(\frac{ra_e - a_i}{r} \right) \right] \omega^2 \\ & + \alpha \left((a_e - a_i) - k^2 \left(\frac{r^2 a_e - a_i}{r^2} \right) \right) = 0. \end{aligned} \quad (4.24)$$

Thus, a Turing-Hopf bifurcation can occur if the parameters satisfy (4.24) with $\omega \neq 0$. In Fig.4, the Turing-Hopf bifurcation curves are shown. Fig.5 displays the space-time pattern of the corresponding Turing-Hopf bifurcation. Here, the values of r and ν are chosen on the Turing-Hopf bifurcation curve in Fig.4(d).

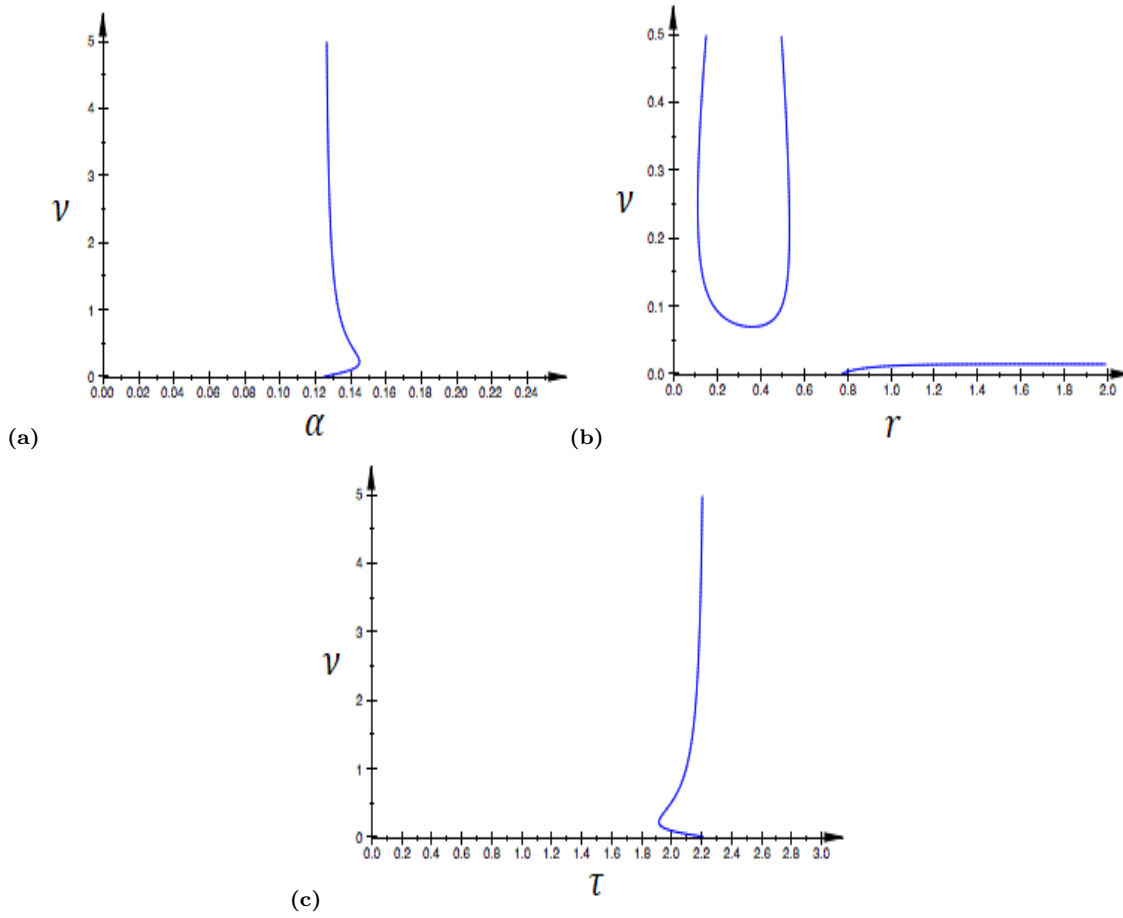


Figure 4: The curves in panels (a)-(c) represent the Turing Hopf bifurcation curves in (4.24) in the α - ν , r - ν , and τ - ν planes, respectively. Parameter values are: (a) $\tau = 2.0$, $r = 0.5$; (b) $\alpha = 0.14$, $\tau = 2.0$; (c) $\alpha = 0.14$, $r = 0.5$. The remaining parameters are fixed at $a_e = 25.0$, $a_i = ra_e$, $c = 15.0$, $v_0 = 0.55$, $\beta := \alpha c \tau F'(v_0)$, $k = 1$, and $\omega = 0.25$.

5 Concluding remarks

In this paper we have studied the bifurcation behavior and the wave patterns generated by a neural field equation with an exponential temporal kernel. The exponential temporal kernel in (2.2) takes into account the finite memory of past activities of the neurons, which the Green's function that was utilized in [16] does not.

Our first observation was that static bifurcations such as saddle-node and pitchfork bifurcations, and static Turing patterns are not possible with an exponential temporal kernel, because the characteristic polynomial does not have an eigenvalue 0. This is in contrast to [16], where the temporal kernel was taken as the Green's function rather than an exponential function, and thus allowed zero eigenvalues.

The dynamic bifurcations, however, turn out to be interesting. In the analysis of the dynamic bifurcations of the equilibrium solution, we have obtained the conditions for the occurrence of Hopf and Turing-Hopf bifurcations. Furthermore, we have numerically illustrated these dynamic bifurcations with bifurcation diagrams and space-time patterns.

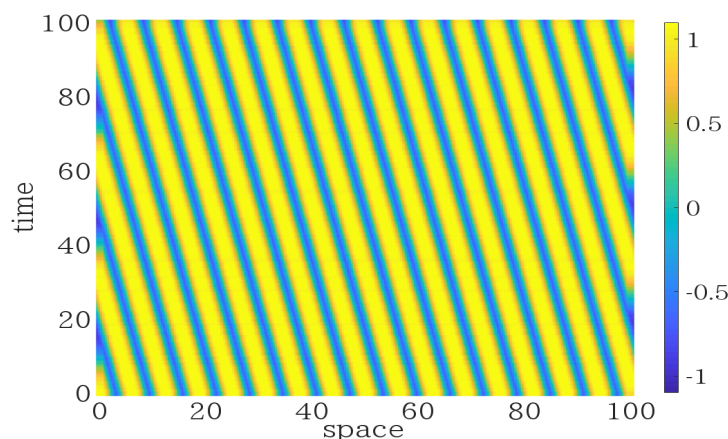


Figure 5: Space-time plot color coded by the membrane potential $v(x, t)$ of the Turing-Hopf instability leading to periodic oscillations of spatially and temporally non-constant solutions, obtained for the Gaussian connectivity kernel. In this plot the excitatory synaptic weight is set at $a_i = 15.0$. The color-bar shows the membrane potential $v(x, t)$. Initial conditions are chosen randomly from a uniform distribution on $[v_0 - 0.1, v_0 + 0.1]$. Parameter values are $\tau = 2.0$, $\alpha = 0.14$, $c = 15.0$, $r = 0.5$, $\nu = 0.11$, $k = 1$, and $a_e = ra_i$.

Acknowledgements This work was supported by the Max-Planck-Institut für Mathematik in den Naturwissenschaften, Leipzig, Germany.

References

1. E.R. Kandel, J.H. Schwartz, T.M. Jessell, Department of Biochemistry, Molecular Biophysics Thomas Jessell, S. Siegelbaum, A.J. Hudspeth, Principles of neural science, vol 4, McGraw-hill, New York, 2000.
2. H.R. Wilson, J.D. Cowan, A mathematical theory of the functional dynamics of cortical and thalamic nervous tissue, Biol. Cybernet. 13 (1973) 55-80.
3. H.R. Wilson, J.D. Cowan, Excitatory and inhibitory interactions in localized populations of model neurons, Biophys. J. 12 (1972) 1-24.
4. S.-I. Amari, Dynamics of pattern formation in lateral-inhibition type neural fields, Biol. Cybernet. 27 (1977) 77-87.
5. R. Veltz, O. Faugeras, Stability of the stationary solutions of neural field equations with propagation delays, J. Math. Neurosci. 1 (2011) 1.
6. L.I. Perlovsky, Toward physics of the mind: Concepts, emotions, consciousness, and symbols, Phys. Life Rev. 3 (2006) 23-55.
7. J. Alswaihi, R. Potthast, I. Bojak, D. Saddy, A. Hutt, Kernel reconstruction for delayed neural field equations, J. Math. Neurosci. 8 (2018) 3.
8. A.H. Abbassian, M. Fotouhi, M. Heidari, Neural fields with fast learning dynamic kernel, Biol. Cybernet. 106 (2012) 15-26.
9. P.C. Bressloff, Spatiotemporal dynamics of continuum neural fields, J. Phys. A. Math. Theor. 45 (2011) 033001.
10. H. Haken, Brain dynamics: an introduction to models and simulations, Springer-Verlag, Berlin, 2007.
11. J. Karbowski, N. Kopell, Multispikes and synchronization in a large neural network with temporal delays, Neural Comput. 12 (2000) 1573-1606.

12. L.G. Morelli, G. Abramson, M.N. Kuperman, Associative memory on a small-world neural network, *Eur. Phys. J. B* 38 (2004) 495-500.
13. T. Prager, L.S. Geier, Stochastic resonance in a non-markovian discrete state model for excitable systems, *Phys. Rev. Lett.* 91 (2003) 230601.
14. M. Spiridon, W. Gerstner, Effect of lateral connections on the accuracy of the population code for a network of spiking neurons, *Network* 12 (2001) 409-421.
15. W. Gerstner, W. Kistler, *Spiking neuron models*, Cambridge Univ. Press, 2002.
16. F.M. Atay, A. Hutt, Stability and bifurcations in neural fields with finite propagation speed and general connectivity, *SIAM J. Appl. Math.* 65 (2004) 644-666.
17. F.M. Atay, A. Hutt, Neural fields with distributed transmission speeds and long-range feedback delays, *SIAM J. Appl. Dyn. Syst.* 5 (2006) 670-698.
18. A. Hutt, F.M. Atay, Analysis of nonlocal neural fields for both general and gamma-distributed connectivities, *Physica D* 203 (2005) 30-54.
19. A. Hutt, F.M. Atay, Effects of distributed transmission speeds on propagating activity in neural populations, *Phys. Rev. E* 73 (2006) 021906.
20. J. Senk, K. Korvasová, J. Schuecker, E. Hagen, T. Tetzlaff, M. Diesmann, M. Helias, Conditions for traveling waves in spiking neural networks, arXiv preprint [arXiv:1801.06046](https://arxiv.org/abs/1801.06046) (2018).
21. M. Polner, J.J.W. Van der Vegt, S.V. Gils, A space-time finite element method for neural field equations with transmission delays, *SIAM J. Sci. Comput.* 39 (2017) B797-B818.
22. O. A. Arqub, Adaptation of reproducing kernel algorithm for solving fuzzy fredholm-volterra integrodifferential equations, *Neural Comput. Appl.* 28 (2017) 1591-1610.
23. O. Faugeras, J. Inglis, Stochastic neural field equations: a rigorous footing, *J. Math. Biol.* 71 (2015) 259-300.
24. J. Rankin, D. Avitabile, J. Baladron, G. Faye, D.J. Lloyd, Continuation of localized coherent structures in nonlocal neural field equations, *SIAM J. Sci. Comput.* 36 (2014) B70-B93.
25. J. Fang, G. Faye, Monotone traveling waves for delayed neural field equations, *Math. Models Methods Appl. Sci.* 26 (2016) 1919-1954.
26. M. Breakspear, Dynamic models of large-scale brain activity, *Nat. Neurosci.* 20 (2017) 340.
27. D.J. Pinto and G.B. Ermentrout, Spatially structured activity in synaptically coupled neuronal networks: I. traveling fronts and pulses, *SIAM J. Appl. Math.* 62 (2001) 206-225.
28. S. Coombes, N. Venkov, L. Shiau, I. Bojak, D.T. Liley, C.R. Laing, Modeling electrocortical activity through improved local approximations of integral neural field equations, *Phys. Rev. E* 76 (2007) 051901.
29. A. Hutt, M. Bestehorn, T. Wennekers, Pattern formation in intracortical neuronal fields, *Network* 14 (2003) 351-368.
30. S.E. Folias, P.C. Bressloff, Breathers in two-dimensional neural media, *Phys. Rev. Lett.* 95 (2005) 208107.
31. C.R. Laing, Spiral waves in nonlocal equations, *SIAM J. Appl. Dyn. Syst.* 4 (2005) 588-606.
32. S.E. Folias, P.C. Bressloff, Breathing pulses in an excitatory neural network, *SIAM J. Appl. Dyn. Syst.* 3 (2004) 378-407.
33. N.A. Venkov, S. Coombes, P.C. Matthews. Dynamic instabilities in scalar neural field equations with space-dependent delays. *Physica D* 232 (2007) 1-15.
34. J. Touboul, Mean-field equations for stochastic firing-rate neural fields with delays: Derivation and noise-induced transitions, *Physica D* 241 (2012) 1223-1244.
35. I. Bojak, D.T. Liley, Axonal velocity distributions in neural field equations. *PLoS Comput. Biol.* 6 (2010) e1000653.
36. A. Hutt, A. Longtin, L. Schimansky-Geier, Additive noise-induced turing transitions in spatial systems with application to neural fields and the Swift-Hohenberg equation. *Physica D* 237 (2008) 755-773.

-
37. S. Coombes, Waves, bumps, and patterns in neural field theories. *Biol. Cybernet.* 93 (2005) 91-108.